Gene expression profiling reveals the heterogeneous transcriptional activity of *Oct3/4* and its possible interaction with *Gli2* in mouse embryonic stem cells

Yanzhen Li [a,b], Jenny Drnevich [c], Tatiana Akraiko [c], Mark Band [c], Dong Li [b,d], Fei Wang [b,d], Ryo Matoba [e], Tetsuya S. Tanaka [a,b,f,g,*]

[a] Department of Animal Sciences, University of Illinois at Urbana–Champaign, Urbana, IL 61801, USA
[b] Institute for Genomic Biology, University of Illinois at Urbana–Champaign, Urbana, IL 61801, USA
[c] The W.M. Keck Center for Comparative and Functional Genomics, University of Illinois at Urbana–Champaign, Urbana, IL 61801, USA
[d] Department of Cell and Developmental Biology, University of Illinois at Urbana–Champaign, Urbana, IL 61801, USA
[e] DNA Chip Research Inc., Yokohama, Kanagawa 230-0045, Japan
[f] Department of Biological Sciences, University of Notre Dame, Notre Dame, IN 46556, USA
[g] Department of Chemical and Biomolecular Engineering, University of Notre Dame, Notre Dame, IN 46556, USA

ARTICLE INFO

ABSTRACT

We examined the transcriptional activity of *Oct3/4* (*Pou5f1*) in mouse embryonic stem cells (mESCs) maintained under standard culture conditions to gain a better understanding of self-renewal in mESCs. First, we built an expression vector in which the *Oct3/4* promoter drives the monocistronic transcription of Venus and a puromycin-resistant gene via the foot-and-mouth disease virus self-cleaving peptide T2A. Then, a genetically-engineered mESC line with the stable integration of this vector was isolated and cultured in the presence or absence of puromycin. The cultures were subsequently subjected to Illumina expression microarray analysis. We identified approximately 4600 probes with statistically significant differential expression. The genes involved in nucleic acid synthesis were overrepresented in the probe set associated with mESCs maintained in the presence of puromycin. In contrast, the genes involved in cell differentiation were overrepresented in the probe set associated with mESCs maintained in the absence of puromycin. Therefore, it is suggested with these data that the transcriptional activity of *Oct3/4* fluctuates in mESCs and that *Oct3/4* plays an essential role in sustaining the basal transcriptional activities required for cell duplication in populations with equal differentiation potential. Heterogeneity in the transcriptional activity of *Oct3/4* was dynamic. Interestingly, we found that genes involved in the hedgehog signaling pathway showed unique expression profiles in mESCs and validated this observation by RT-PCR analysis. The expression of *Gli2*, *Ptch1* and *Smo* was consistently detected in other types of pluripotent stem cells examined in this study. Furthermore, the Gli2 protein was heterogeneously detected in mESC nuclei by immunofluorescence microscopy and this result correlated with the detection of the Oct3/4 protein. Finally, forced activation of *Gli2* in mESCs increased their proliferation rate. Collectively, it is suggested with these results that *Gli2* may play a novel role in the self-renewal of pluripotent stem cells.

© 2013 Elsevier Inc. All rights reserved.

1. Introduction

Embryonic stem cells (ESCs) are derived from preimplantation embryos and are capable of both long-term proliferation (self-renewal) and differentiation into cell types of all three germ layers (pluripotency). The self-renewal and pluripotency of ESCs are sustained by a combination of essential transcription factors [1] and the extracellular signals that drive the expression of these transcription factors [2]. Recent studies have observed that undifferentiated mouse ESC (mESC) cultures contain multiple cell populations showing fluctuating expression levels of genes associated with cellular pluripotency and cell differentiation [3–18]. Cellular pluripotency and cell differentiation genes are downregulated or expressed in approximately one-tenth of cells in steady state culture (for a review, see [19–22]). For example, when mESCs were sorted into *Zscan4*-positive and *Zscan4*-negative subpopulations based on expression levels, the subpopulations were able to regain *Zscan4*-negative and *Zscan4*-positive cells, respectively, when they were replated and cultured separately [11]. Interestingly, the constitutive knockdown of *Zscan4* significantly decreased telomere length, whereas its constitutive expression increased the levels of telomeric sister chromatid exchange (T-SCE; [11]). Both telomere shortening and increased T-SCE rates lead to acceleration of the replicative senescence [23,24].

Therefore, the heterogeneous expression of *Zscan4* is necessary for mESCs to self-renew indefinitely.

In studies with other genes [3,5,12–16,18], each subpopulation has exhibited unique differentiation potential. For example, *Nanog*-high mESCs are resistant to differentiation, whereas *Nanog*-low mESCs are prone to differentiation [3]. Consequently, the presence of subpopulations in mESC cultures typifies the plasticity of early embryonic cells and dynamically sustains their self-renewal and pluripotency. The autorepressive feedback of Nanog [25], extrinsic TGFβ signaling pathways, such as Nodal and BMP [26], and activity of the basic-helix–loop–helix transcription factor Tcf15 [16] are responsible for maintaining heterogeneous *Nanog* expression in mESC cultures. In addition, the stiffness of the culture dishes [27] and/or the uneven partition of the cytoplasm during cell division [28,29] may contribute to the variable expression of these genes in mESC cultures. However, the underlying molecular mechanism that is responsible for transcriptional heterogeneity in mESCs remains elusive.

In this study, we generated a genetically-engineered mESC line to examine its self-renewal. The mESC line contains an expression cassette with an *Oct3/4* (*Pou5f1*) promoter that drives the monocistronic expression of Venus and a puromycin-resistant gene product. The mESCs were cultured under standard conditions with or without puromycin (puromycin-positive and puromycin-negative cultures, respectively) and subjected to Illumina expression microarray analysis. It is suggested with these data that mESCs exhibit fluctuations in *Oct3/4* expression levels and that *Oct3/4* plays an essential role in sustaining the basal transcriptional activities required for duplication of cells with equal differentiation potential. Surprisingly, we found that the genes involved in the hedgehog signaling pathway, i.e., *Gli2* and *Ptch1*, showed unique expression profiles in mESCs. It is suggested with our results that *Gli2* may play a novel role in the self-renewal of pluripotent stem cells.

2. Materials and methods

2.1. Vector construction

Standard molecular cloning techniques were used to build pOctV2AP in which the *Oct3/4* promoter drives the expression of Venus [17,30] and pCAG_Gli2ERP from which the protein coding sequence of *Gli2* is expressed as a fusion protein with the human estrogen receptor ERT2 [31,32]. A stepwise description of the vector construction is provided in the Supplementary Materials and methods.

2.2. Cell culture

Mouse embryonic stem cells (mESCs; OGR1 and W4) were cultured under standard conditions, as described previously [27,33,34]. Briefly, mESCs were plated on 0.1% gelatin-coated tissue culture dishes and cultured in Dulbecco's modified Eagle's medium (high glucose; Life Technologies, Carlsbad, CA) supplemented with 15% fetal bovine serum (FBS; Life Technologies, and Gemini Bio-Products, West Sacramento, CA), 0.1 mM non-essential amino acids (Life Technologies), 2 mM GlutaMax I (Life Technologies), 1 mM sodium pyruvate (Life Technologies), 100 U/ml penicillin and 0.1 mg/ml streptomycin (Sigma-Aldrich, St. Louis, MO), 0.1 mM 2-mercaptoethanol (Sigma-Aldrich) and 1000 U/ml Leukemia inhibitory factor (LIF; EMD Millipore, Billerica, MA). To determine the best serum lot for mESC culture, several different serum lots from a few different companies were tested by plating mESCs at a low density under 15 or 30% serum conditions. Although three serum lots contributed to the results presented in this manuscript due to the duration of the study, heterogeneity in the expression of the *Oct3/4* reporter was consistently observed. To expand mESCs at 80% confluence, TrypLE Express (Life Technologies) and the same volume of the standard culture medium were sequentially added to the culture and a single cell suspension was prepared. The plating density was 1:5. Under these conditions, it took two days for mESCs to reach 80%

confluence after plating. More than 80% of the mESCs exhibited an appearance of undifferentiated cells under these conditions. Mouse teratocarcinoma cell lines (F9 and P19 [35,36]), which were kindly provided by Dr. Minoru S. H. Ko, National Institute on Aging/NIH, were cultured under standard conditions for mESCs without LIF.

pOctV2AP (see Supplementary Materials and methods) was linearized with BspHI and delivered by electroporation into feeder-free W4 ESCs at passage 15 (10 μg DNA/1.0×10^7 cells/cuvette, 0.8 kV/cm, 12 pulses of 99 μs/pulse, BTX ECM200). After selection with 2 μg/ml puromycin (InvivoGen, San Diego, CA) for 11 days, the drug-resistant colonies, designated OVW4, were collected (passage 1) and expanded. The OVW4 cells were maintained under standard conditions and sorted at passage 18 based on fluorescence at 575 nm, as described previously [27].

Linear pCAG_Gli2ERP digested with ScaI (0.5, 3 and 4 μg) was nucleofected into OGR1 mESCs (at passages 21, 25 and 12, respectively) according to the manufacturer's instruction (Lonza, Basel, Switzerland). Stable lines (referred to as Gli2ER hereafter) were isolated 10–14 days after selection with 2 μg/ml puromycin supplemented in the standard culture medium. Gli2ER clones were maintained and assayed in the presence of puromycin within 10 passages after isolation. After trypsinization, the same volume of a single cell suspension was plated into two sets of gelatin-coated wells of 24-well plates in the standard culture medium. Roughly 100–3000 cells were plated in this manner. One day after plating, one set of the wells were fed with the standard medium supplemented with 20 nM 4-hydroxytamoxifen (4OHT; T176, Sigma-Aldrich). We determined that 20 nM 4OHT was optimum: when a higher dose was applied to culture, OGR1 mESCs decreased the proliferation rate (data not shown). Four days after the 4OHT treatment, a single cell suspension was prepared using an electronic pipet (Biohit, Bohemia, NY) to reduce pipetting errors, although the final volume of the single cell suspension was measured using a pipetman (Eppendorf, Hauppauge, NY). The number of cells (larger than 8.4 μm and smaller than 33.6 μm in diameter) was counted using Scepter™ (Millipore). Results were statistically analyzed using one-tail Student's t-test.

The dynamic of *Oct3/4* reporter expression was examined using mESCs that express EGFP under the *Oct3/4* promoter, namely OGR1 [27,33,34,37]. After a single cell suspension was diluted with the standard culture medium, EGFP expression levels in each OGR1 mESC were determined under an inverted microscope (Leica DMI4000B) equipped with an epifluorescent lamp. Single OGR1 mESCs were individually plated in each well of a gelatin-coated 96-well plate (Sarstedt AG & Co., Nümbrecht, Germany) filled with the standard culture medium by the single cell manipulation method [38,39]. Five to seven days after plating, the plating efficiency and the morphology and EGFP expression of colonies developed from single OGR1 mESCs were measured. Images were processed using ImageJ and enhanced in the same way. For this set of experiments, OGR1 mESCs were used at passages 6–19.

2.3. Microarray hybridization and analysis

One day after a subclone of OVW4, namely A02 (at passage 5), was plated at 100 cells/cm², it was maintained under the presence or absence of puromycin (2 μg/ml; Invivogen) for 4 days. Total RNA was extracted from 3 separate dishes per condition and subjected to microarray analysis (MouseWG-6 v1.1 Expression BeadChips; Illumina Inc., San Diego, CA). More detailed descriptions of the microarray hybridization and data analysis are provided in the Supplementary Materials and methods.

After background correction and quantile normalization, the log2-transformed data were assessed for differential expression. We arbitrarily considered genes with a false discovery rate [40] less than 0.05 and a fold-change of 1.2 or greater differentially expressed. Then, a list of differentially expressed genes with an expression level of 200 or greater in the puromycin-positive OVW4 culture was generated. A

scatter plot and a heat map were constructed using Microsoft Excel and MultiExperiment Viewer [41,42], respectively. ConPath Navigator (http://conpath.dna-chip.co.jp/; DNA Chip Research Inc., Yokohama, Kanagawa, Japan) was used to compare this gene list with published data [42,43], and GOToolBox (http://genome.crg.es/GOToolBox/; [44]) was used to investigate its associated gene annotations.

2.4. Semi-quantitative (sq) and quantitative (q) RT-PCR

The 1.6 μg of total RNA extracted from stem cells in each culture condition was used to synthesize the first cDNA strand, as described previously [27,45,46]. For gene expression analysis of undifferentiated and differentiated mESCs, OGR1 was plated at 100 cells/cm^2 and maintained in the presence or absence of LIF for 4 days under standard conditions with animal serum. PCR mixtures were prepared using Phusion DNA polymerase (New England Biolab, Ipswich, MA), according to the manufacturer's instructions. The PCR conditions were as follows: initial denaturing at 98 °C for 1 min followed by 25 cycles of denaturing at 98 °C for 10 s, annealing at 65 °C for 30 s, extension at 72 °C for 30 s and a final extension at 72 °C for 7.5 min. The primer sets used for this study were described previously [5,27,33,34,45,47,48] or are listed in Supplementary Table 1. To quantify relative gene expression, images of ethidium bromide-stained PCR products in agarose gels were analyzed using ImageJ. An identical rectangular selection was used to measure the mean fluorescence intensity of each PCR product as well as a local background level near the product per image. After background subtraction, values were divided by the one of Smo as a reference to obtain relative gene expression levels.

Quantitative (q) RT-PCR was carried out essentially as described previously [34], except that the One-Step qRT-PCR kit (Life Technologies) was used.

2.5. Immunofluorescence microscopy

After fixation with 4% paraformaldehyde (Sigma-Aldrich) in PBS at room temperature for 15 min, mESCs cultured on glass-bottom dishes (MatTek corporation, Ashland, MA) coated with 0.15 mg/ml type IA collagen (Nitta Gelatin Co., Osaka, Japan) were washed with PBS and blocked with 0.1% Triton X-100 at room temperature for 10 min. After PBS washes, these mESCs were incubated with 10% Image-iT FX signal enhancer (Life Technologies) at room temperature for 30 min, followed by incubation with a mouse anti-human Oct4 monoclonal antibody (sc-5279, Santa Cruz Biotechnology, Santa Cruz, CA) and a rabbit anti-human Gli2 polyclonal antibody (ab26056, Abcam, Cambridge, MA) diluted with 10% Image-iT FX signal enhancer at a 1:200 ratio at 4 °C overnight. After PBS washes, the samples were incubated with goat Alexa Fluor 488 anti-mouse IgG and goat Alexa Fluor 568 anti-rabbit IgG polyclonal antibodies (Life Technologies) diluted in 10% Image-iT in PBS at room temperature for 1 h. Cellular nuclei were stained with Hoechst 33258 (0.2 mg/ml; Sigma) after PBS washes. The immunostained mESCs were treated with ProLong Gold antifade reagent (Life Technologies) overnight. A confocal microscope LSM 700 was used. Image analysis was carried out using ImageJ. Mean fluorescence intensity values that are greater than 40 and 20 are considered positive for the expression of Oct3/4 and Gli2, respectively (see Supplementary Fig. 1).

Detection of the SSEA1 antigen [49] was carried out using the FITC-conjugated anti-SSEA1 antibody (sc-21702, Santa Cruz Biotechnology) under the standard fluorescence microscopy (Observer.Z1, Zeiss) essentially as described previously [34,27].

3. Results and discussion

3.1. Mouse embryonic stem cells showed fluctuating expression of Oct3/4

To examine the transcriptional activity of Oct3/4 in mESCs cultured under standard conditions with animal serum (referred to as standard conditions hereafter), the Oct3/4 promoter [50] was cloned and used to build a fluorescent reporter construct, namely pOctV2AP (Fig. 1A; see Supplementary Materials and methods). In this construct, the Oct3/4 promoter drives the expression of Venus, a variant of yellow fluorescent protein [30], which is co-expressed with a puromycin-resistant gene product via the self-cleaving peptide T2A [51]. After pOctV2AP was linearized and delivered to mESCs by electroporation, mESC clones that exhibited puromycin resistance were isolated. As a proof of principle, these mESC clones, referred to as OVW4, expressed Venus under standard culture conditions (Fig. 1B). Interestingly, Venus expression was not detected in all of the OVW4 mESCs under standard culture conditions (Fig. 1B), i.e., Venus exhibited a variable expression pattern across OVW4 mESCs. In contrast, Venus fluorescence was relatively uniform when OVW4 cells were cultured in the presence of puromycin (Fig. 1C). Thus, these results indicate that the transcriptional activity of Oct3/4 fluctuates in mESCs under standard culture conditions. Heterogeneity in the transcriptional activity of Oct3/4 is not under the influence of animal serum because we observed similar heterogeneous expression of the Oct3/4 reporter in mESCs maintained under chemically-defined serum-free conditions [33,52] (Supplementary Fig. 2). Flow cytometric analysis revealed that approximately one-fifth of the OVW4 cells maintained under standard conditions lacked Venus expression (data not shown). When OVW4 cells were introduced into host blastocysts, Venus was fluorescently detected in the testes of developing fetuses at embryonic day 17.5 (Fig. 1D), thus validating the promoter activity of the transgene.

Next, the expression of genes associated with cellular pluripotency (Oct3/4, Esg1(Dppa5a), Fgf4, Nanog, Rex1 and Sox2) and cell differentiation (Rhox6, Rhox9 and Tcf15) were examined in Venus-positive and Venus-negative OVW4 cells by semi-quantitative reverse transcriptase polymerase chain reaction (sqRT-PCR; Fig. 1E). Nanog, Rex1, Rhox6/9 and Tcf15 are known to be heterogeneously expressed in mESCs [3–6,16,45]. Notably, Venus-negative OVW4 cells exhibited a marked downregulation of Fgf4, Rex1, Sox2, Rhox9 and Tcf15, whereas Esg1, Nanog and Rhox6 expression levels were roughly maintained in Venus-negative OVW4 cells (Fig. 1E). Therefore, multiple subpopulations of mESCs existed in the culture, as suggested previously [4].

We investigated whether or not the observed heterogeneity in the transcriptional activity of Oct3/4 is dynamic. Initially, single OVW4 mESCs were plated, but their recovery was poor due to W4's high dependency on LIF [53]. Therefore, R1 mESCs that express EGFP under the Oct3/4 promoter (OGR1 [27,33,34,37]) were used. Single EGFP-high or low OGR1 mESCs were plated into each well of 96-well plates and maintained under standard conditions (Figs. 2A–C). Five to seven days after plating, 42.8% of EGFP-high and 36.6% of EGFP-low single OGR1 mESCs grew into individual colonies ($p > 0.05$). The appearance of each colony was arbitrarily categorized into the following three: a dome-like shape with bright EGFP fluorescence indicative of pluripotent mESCs, a flattened shape with moderate EGFP fluorescence indicative of reduced differentiation potential and a committed cell shape with reduced EGFP fluorescence indicative of cell differentiation (Figs. 2D–I). EGFP-low mESCs produced slightly more colonies with an appearance of committed cells (38.1%) than EGFP-high mESCs (34.3%) at the expense of dome-like colonies (28.6% in EGFP-low mESCs vs. 33.1% in EGFP-high mESCs; Fig. 2J). However, this result shows no statistical significance and both EGFP-high and EGFP-low mESCs formed colonies with heterogeneous EGFP expression. Thus, we conclude that heterogeneity in the transcriptional activity of Oct3/4 is dynamic.

3.2. Microarray analysis revealed global transcriptional heterogeneity in mouse embryonic stem cells

To evaluate the transcriptional heterogeneity in mESCs at a genomic scale, OVW4 cells were maintained under standard conditions in the presence or absence of puromycin, and subjected to expression microarray analysis (Fig. 3A). Hybridization experiments were carried out in
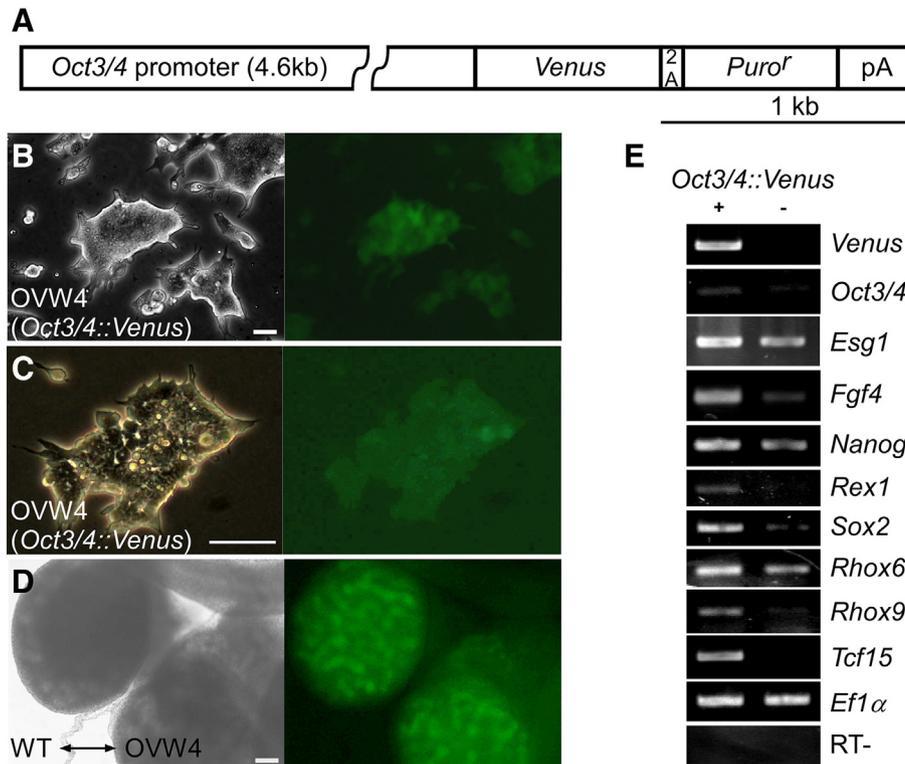
Fig. 1. Characterization of OVW4 mouse embryonic stem cells (mESCs). (A) A schematic representation of the expression cassette used to generate OVW4 mESCs. The *Oct3/4* promoter drives the monocistronic transcription of the Venus fluorescent protein and a puromycin-resistant gene product (puromycin-N-acetyltransferase; *Puro*[r]) via T2A (2A). pA, the bovine growth hormone polyadenylation signal. The bar denotes a length of 1 kb. (B–D) Bright (left) and dark (right) field images are shown. Bars, 50 μm in B and C and 100 μm in D. (B) A mESC line that harbors the Venus_T2A_Puro[r] cassette driven by the *Oct3/4* promoter (*Oct3/4::Venus*) was designated OVW4 and maintained under standard conditions (left). Venus showed fluctuating expression (right). (C) OVW4 was maintained under standard conditions supplemented with puromycin (left). Venus showed relatively homogeneous expression (right). (D) Fetal testes were isolated from a chimera at embryonic day 17.5, which was derived from injection of OVW4 into a host blastocyst (left). The expression of Venus was detected in seminiferous tubules (right). (E) Undifferentiated OVW4 was sorted according to Venus expression levels at 575 nm and subjected to first strand cDNA synthesis. The cDNA obtained from Venus-positive (+) or negative (−) OVW4 was used as a template for the subsequent polymerase chain reaction (PCR) with each gene-specific primer pair indicated on the right. *Ef1a* is a positive control, and RT− is a negative control.
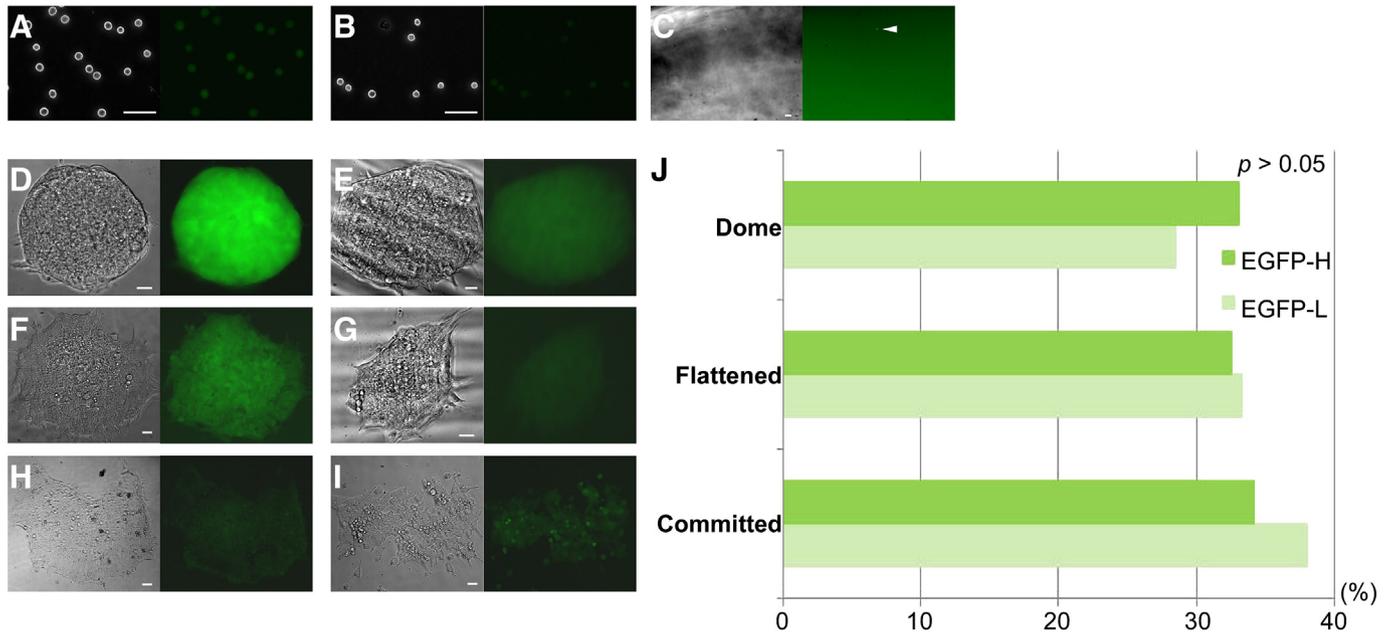

Fig. 2. Heterogeneous expression of the *Oct3/4* reporter is dynamic. (A–I) Phase contrast (left) and fluorescence (right) images of mouse embryonic stem cells (mESCs) that express EGFP under the *Oct3/4* promoter, namely OGR1, are shown. The EGFP fluorescence indicates the transcriptional activity of *Oct3/4*. Bars, 50 μm. (A & B) Single EGFP-high (A) and EGFP-low (B) OGR1 mESCs are shown. (C) An EGFP-high mESC (arrowhead) was plated in a well of a 96-well plate. No other cell exists in the same well. (D–I) Colonies with a dome-like shape (D & E), a flattened shape (F & G) and a committed cell shape (H & I) were formed from single EGFP-high (D, F & H) or EGFP-low (E, G & I) OGR1 mESCs. Note that colonies shown in E and G were formed on the plastic plate showing "grooves" on the opposite side of the bottom due to the manufacturing-associated issue. (J) The frequency of the appearance of a dome-like, flattened or committed cell shape was measured 5–7 days after plating single EGFP-high and EGFP-low mESCs. The total numbers of single cells plated are 181 for EGFP-high and 21 for EGFP-low mESCs from five replications. The Chi-square test showed no statistical significance.
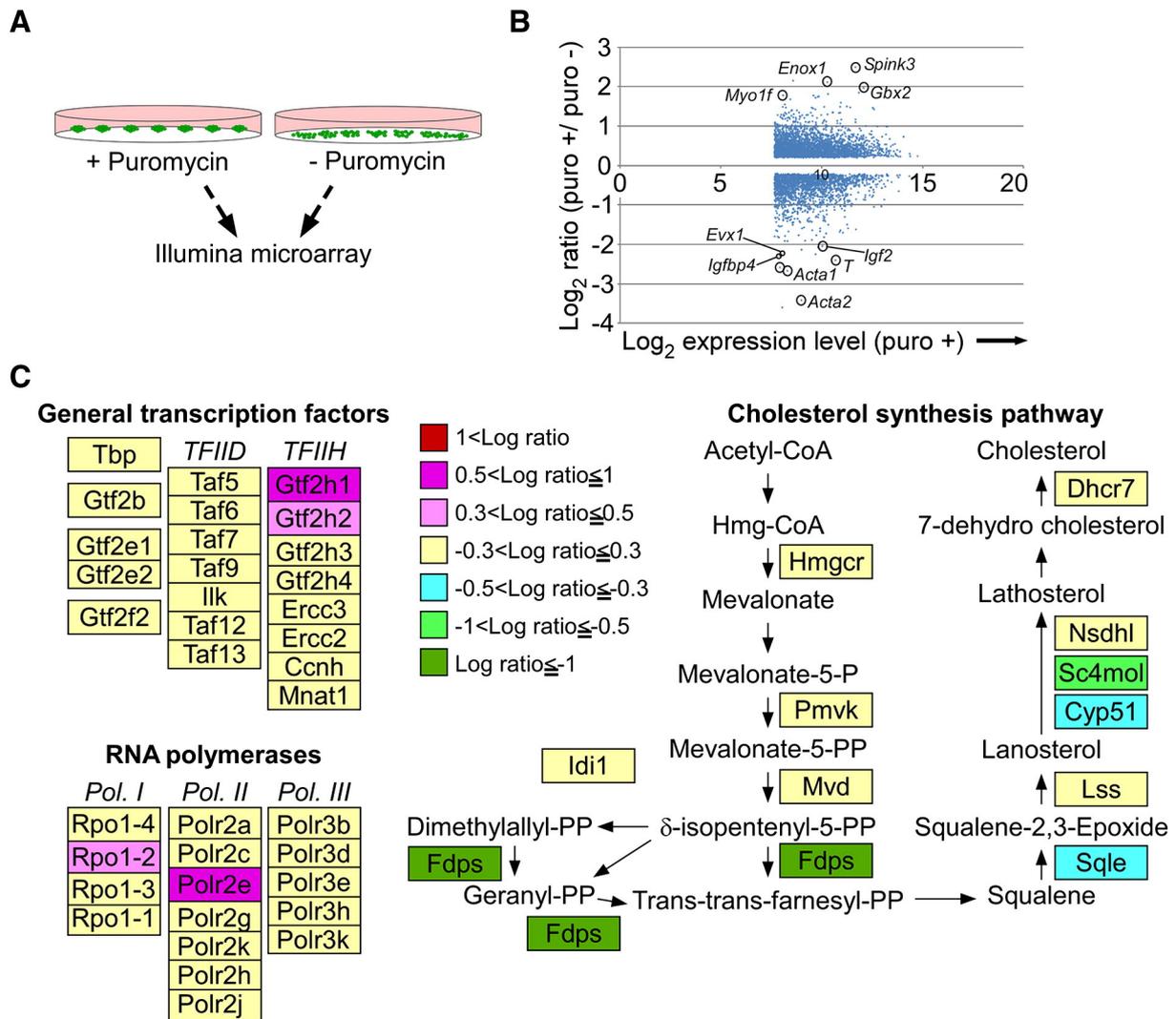
Fig. 3. Global transcriptional heterogeneity in OVW4. (A) A schematic representation of the experimental design. OVW4 mESCs were maintained under standard conditions with or without puromycin, and subjected to Illumina expression microarray analysis. (B) A scatter plot of the 4606 probes exhibiting differential expression between OVW4 maintained in the presence or absence of puromycin (referred to as puro+ or puro−, respectively). Differential expression was defined by arbitrarily determined cut-off values (see Section 2.3 in Materials and methods). For each probe, the log2-transformed average expression level of hybridizations for puro+ (collected in triplicate) was plotted on the x-axis and the log2-transformed ratio of expression levels between puro+ and puro− ("puro+/puro−") was plotted on the y-axis. Probes representing indicated genes are marked on the plot. (C) Two representative pathways that exhibited significant enrichment of genes highly expressed in puro+ (left, general transcriptions factors and RNA polymerases) or puro− (right, cholesterol synthesis) are shown. The color of each box represents the normalized levels of fold-differences in gene expression between puro+ and puro−, as indicated in the legend.

triplicate for each condition. A total of 4606 probes were selected as differentially expressed based on their statistical confidence (see Section 2.3 in Materials and methods). In the puromycin-positive OVW4 culture, 2717 probes were overexpressed, whereas 1889 probes were underexpressed (the gene list is available in Supplementary Table 2). The variation in gene expression levels between puromycin-positive and puromycin-negative conditions was evident in a scatter plot (Fig. 3B). Among the variably expressed genes, *Spink3*, which encodes a serine peptidase inhibitor, showed the largest fold induction in OVW4 cells grown in the presence of puromycin. In addition to *Spink3*, expression levels of *Enox1*, *Gbx2* and *Myo1f* were upregulated when OVW4 cells were maintained in the presence of puromycin (Fig. 3B). These four genes were consistently downregulated when the *Oct3/4* expression level was knocked-down [54]. Genes associated with the self-renewal and pluripotency of mESCs, such as *Dppa2*, *Dppa4*, *Eras*, *Fbxo15*, *Mybl2*, *Sox2* and *Utf1*, were enriched in OVW4 cells that were cultured in the presence of puromycin, whereas genes associated with cell differentiation, such as *Acta1*, *Acta2*, *Evx1*, *Hes1*, *Igf2*, *Igfbp4*, *Lefty2*, *Msx1*, *Notch3*, *Pitx2* and *T*, were under-represented. Collectively, these results indicate that a standard culture of mESCs

contains a cell population with reduced *Oct3/4* transcriptional activity, which leads to the generation of subpopulations with expression profiles that are similar to differentiated cells.

Next, we investigated the gene enrichment and functional annotations associated with this gene list. The enriched probe sets in puromycin-positive OVW4 cultures contained 2368 unique gene symbols, which yielded 1264 functionally annotated genes (53%), whereas enriched probes in puromycin-negative OVW4 cultures contained 1689 unique gene symbols, which included 1034 annotated genes (61%). Uncharacterized genes were enriched in puromycin-positive OVW4 cultures, which may be indicative of a naïve state of undifferentiated cells [55]. Similar results were obtained when mESC gene expression profiles were compared with lineage-committed trophoblast stem cells [47]. By arbitrarily selecting probes with greater than 2-fold expression level differences between the two conditions, the gene lists were reduced to 286 and 365 annotated genes in puromycin-positive and puromycin-negative OVW4 cultures, respectively (Tables 1 and 2). Interestingly, the gene list for the puromycin-positive OVW4 cultures contained genes involved in nucleic acid metabolism (Table 1), whereas genes involved in embryonic development, cholesterol

Table 1
The functional annotations of genes overrepresented in puromycin-positive OVW4 cultures.

Level[a]	Gene Ontology ID	Term	# in the reference[b]	Frequency in the reference	# in the gene list[c]	Frequency in the gene list	p-Value[d]
2	0008152	Metabolic process	7146	0.4875	187	0.6538	0.000006481434
3	0043170	Macromolecule metabolic process	5310	0.3622	147	0.514	0.00006951657
5	0034960	Cellular biopolymer metabolic process	4682	0.3194	141	0.493	0.0000004910301
5, 6	0010468	Regulation of gene expression	2019	0.1377	69	0.2413	0.0012982

[a] The terms at levels 3, 5, and 6 are derived from the parental term at level 2. A total of 24 terms showed statistical significance (see "d" below), although they belong to the same parental term. Only the representative daughter terms are shown.

[b] Gene symbols in Mouse Genome Informatics were used as a reference.

[c] A total of 706 genes exhibiting a 2-fold increase in their expression levels at FDR < 0.05 contain 640 non-redundant gene symbols, of which 286 symbols are functionally annotated.

[d] p-Values were calculated using the hypergeometric test (default setting) and the Bonferroni correction. GO annotations that have p-values less than 0.01 are considered statistically significant.

metabolism, and cytoskeletons were noted on the puromycin-negative gene list (Table 2). Similar results were independently obtained using ConPath Navigator (Fig. 3C; http://conpath.dna-chip.co.jp/). ConPath Navigator is a search tool for genes relative to biological signaling pathways built by GenMAPP [56]. Taken together, it is suggested with these data that Oct3/4 plays an essential role in maintaining basal cellular transcriptional activities while suppressing the expression of genes involved in cell differentiation. This function of Oct3/4 is indicative of a gene that is responsible for regulating the duplication of cells with equal differentiation potential, i.e., self-renewal.

Our expression microarray analysis identified about 2300 annotated genes that potentially exhibit heterogeneous expression under the influence of Oct3/4 in mESCs. This analysis was done using OVW4 cultured in the presence or absence of puromycin under conditions with LIF and animal serum without feeder layers. These conditions might have enriched a population of cells that express Oct3/4 at a very high level (e.g., [57]) and contributed to magnifying the gene list. Interestingly, single-cell gene expression analysis showed that nine genes associated with cellular pluripotency including Nanog and Oct3/4 exhibited variable expression similar to Gapdh [58]. In this analysis, mESCs were maintained under conditions with LIF, animal serum and feeder layers. Under these conditions, fluctuating expression of the nine genes might have been less pronounced than in conditions without feeder layers. However, these two studies clearly demonstrated that gene expression in mESCs is quite variable, so that bulk analysis of gene expression is not suited for understanding the mechanism of cellular pluripotency.

3.3. Undifferentiated pluripotent stem cells expressed genes involved in the hedgehog signaling pathway

Our expression microarray data clearly demonstrate that standard cultures of mESCs consist of heterogeneous populations. Next, we used ConPath Navigator to perform a cross-platform comparison of our current data with published datasets that reported gene expression profiles of mESCs in the course of Oct3/4 downregulation [42,43]. These published datasets were generated using bulk preparations of mESCs maintained under standard conditions. On the other hand, our dataset took into account the heterogeneous transcriptional activity of Oct3/4 in mESCs maintained under similar conditions. Therefore, we aimed at investigating whether our dataset is consistent with or offers alternative interpretations of the published datasets. Because not all of the probes tested in our dataset were necessarily examined in the published datasets, we used two datasets for comparison. Interestingly, we found unique expression patterns in genes that are involved in the hedgehog (Hh) signaling pathway. For example, the transcription factor Gli2 and the transmembrane receptor Ptch1 were consistently highly expressed in mESCs that displayed high transcriptional activity of Oct3/4 (i.e., OVW4 cells that were cultured in the presence of puromycin, "puro+"; Table 3), whereas the transcription repressor Gli3 was highly expressed in OVW4 cells that were cultured in the absence of puromycin ("puro"; Table 3). The expression levels of Gli2, Gli3 and Ptch1 were comparable to that of Sox2, a co-factor of Oct3/4 (Table 3). The forced downregulation of Oct3/4 transcription [43] induced downregulation and up-regulation of Gli2 and Gli3, respectively (Fig. 4A). Thus, the positive correlation between Gli2 and Oct3/4 expression, and the negative correlation between Gli3 and Oct3/4 expression were independently validated. The Ptch1 expression pattern observed in the current dataset was unexpected because, according to Walker et al. [42], Ptch1 expression markedly increased a few days after cell differentiation was induced (by the withdrawal of LIF from the culture or the addition of retinoic acid to the culture), but returned back to its basal level within 5 days [42]. Another study independently reported a similar expression profile of Ptch1 [59]. However, Ptch1 expression became further downregulated when mESCs were differentiated in the absence of LIF but the presence of retinoic acid for 20 days [60]. Ptch1 may be influenced by both LIF and differentiation-inducing signals.

These results were unexpected because the Hh signaling pathway governs cell type specification and embryonic patterning [61]. In

Table 2
The functional annotations of genes overrepresented in puromycin-negative OVW4 cultures.

Level[a]	Gene Ontology ID	Term	# in the reference[b]	Frequency in the reference	# in the gene list[c]	Frequency in the gene list	p-Value[d]
2	0032502	Developmental process	2915	0.1989	112	0.3068	0.0004047
3	0007275	Multicellular organismal development	2476	0.1689	96	0.263	0.0025906
4, 5	0009792	Embryonic development ending in birth or egg hatching	421	0.0287	28	0.0767	0.0030938
2	0010926	Anatomical structure formation	775	0.0529	43	0.1178	0.0007994
4, 5, 6	0034728	Nucleosome organization	96	0.0065	12	0.0329	0.0072877
5, 6, 7	0016125	Sterol metabolic process	78	0.0053	12	0.0329	0.0007878
3, 4, 5	0016192	Vesicle-mediated transport	419	0.0286	28	0.0767	0.0028278

[a] Terms belonging to the same parental term (level 2) are grouped. A total of 15 terms showed statistical significance (see "d" below). Only the representative terms are shown. At least 4 different parental terms (level 2) are expected, although 2 of them did not show statistical significance.

[b] Gene symbols in Mouse Genome Informatics were used as a reference.

[c] A total of 613 genes exhibiting a 2-fold increase in their expression levels at FDR < 0.05 contain 559 non-redundant gene symbols, of which 365 symbols are functionally annotated.

[d] p-Values were calculated using the hypergeometric test (default setting) and the Bonferroni correction. GO annotations that have p-values less than 0.01 are considered statistically significant.

Table 3
The differential expression of genes involved in the Hh signaling pathway in OVW4[a].

Gene symbol	Refseq ID	Entrez ID	FDR	Puro+	Puro−	Log2 (Puro+/−)
(i) Genes showing statistically significant differential expression						
Gli2	NM_001081125.1	14633	0.00	1238	839	0.6
Gli3	NM_008130.2	14634	0.00	1052	1743	−0.7
Igf2	NM_010514.3	16002	0.00	1036	4279	−2.0
Ptch1	NM_008957.2	19206	0.00	1107	494	1.2
Rab23	NM_008999.4	19335	0.01	231	193	0.3
Sap18	NM_009119.3	20220	0.03	268	227	0.2
Smo	NM_176996.4	319757	0.00	226	394	−0.8
Sox2[b]	NM_011443.3	20674	0.00	1016	577	0.8
(ii) Genes that did not show statistical significance or had expression levels less than 200						
Cdk1	NM_007659.3	12534	>0.05	3679	4071	
Crebbp	NM_001025432.1	12914	>0.05	455	540	
Dhh	NM_007857.4	13363	>0.05	<200	<200	
Dyrk1a	NM_007890.2	13548	>0.05	<200	<200	
Ptch2	NM_008958.2	19207	0.00	<200	<200	
Sin3a	NM_011378.2	20466	>0.05	2581	2593	
Ski	NM_011385.2	20481	>0.05	784	692	
Stk36	NM_175031.3	269209	>0.05	<200	<200	
Sufu	NM_015752.2	24069	>0.05	413	426	

[a] The expression microarray did not contain probes for the following genes involved in the Hh signaling pathway: Gas1, Gli1, Ihh and Shh.
[b] Sox2 is not directly involved in the Hh signaling pathway, but it has been listed for comparison.
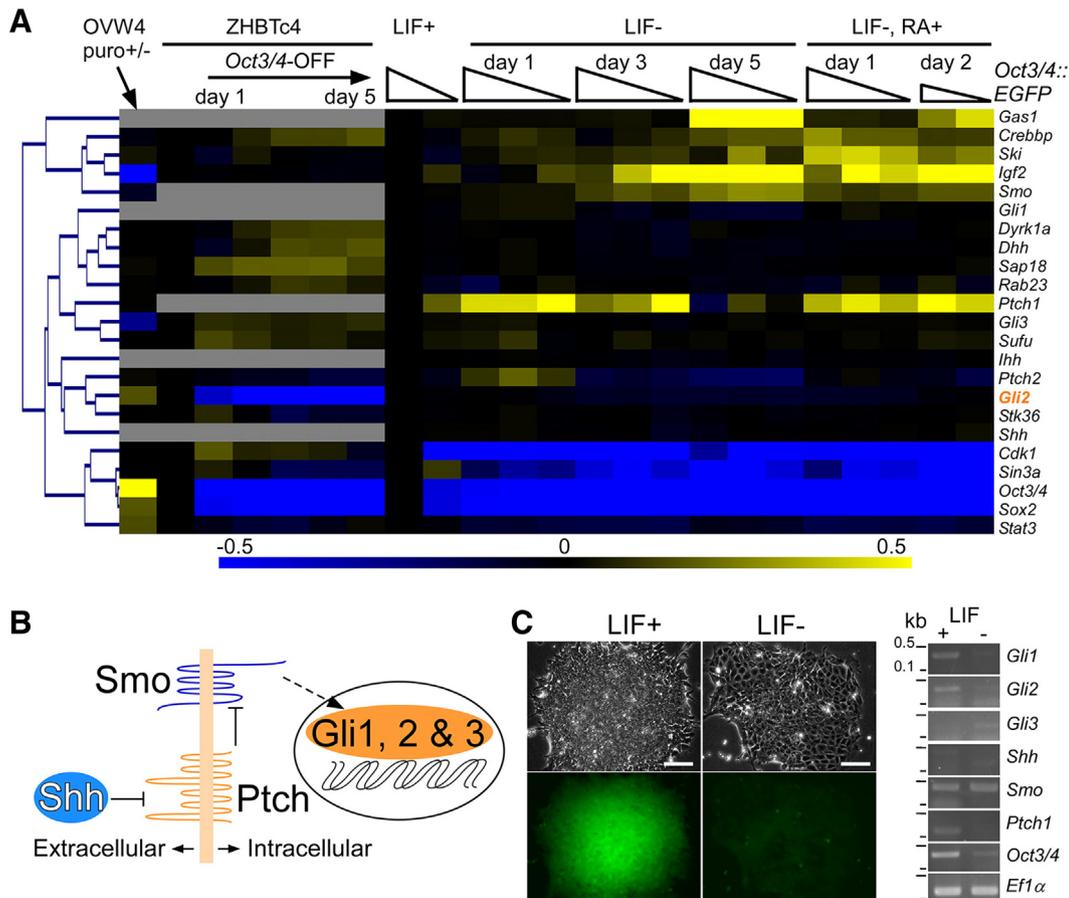

Fig. 4. The expression of genes involved in the hedgehog pathway of mESCs. (A) A heat map of genes (rows) involved in cellular pluripotency and the hedgehog pathway based on present (OVW4 puro+/−) and published (ZHBTc4, LIF+, LIF−, RA+ [41,42]) datasets (columns). ConPath Navigator was used to compare data obtained from multiple platforms. In the published datasets, mESC differentiation was induced by either the forced downregulation of Oct3/4 transgenes using Oct3/4-null mESCs (ZHBTc4 [42]), or the withdrawal of LIF (LIF−) for 5 days and the addition of all-trans retinoic acid (RA+) under the LIF− condition for 2 days using OGR1 mESCs (Oct3/4::EGFP [41]). The triangles indicate the level of EGFP expression in OGR1. The color scale indicates relative gene expression levels. Missing values are shaded in gray. (B) A schematic representation of the Sonic hedgehog (Shh) pathway. Without the growth factor Shh, the Shh receptor Patched (Ptch) represses Smoothened (Smo). When Shh binds to Ptch, Shh represses Ptch, allowing activation of Smo. Subsequently, Smo can activate protein activity of transcription factors Gli1, Gli2 and Gli3. (C) The expression of genes shown in B was examined in undifferentiated (LIF+, left) and differentiated (LIF−, middle) OGR1 mESCs. Phase contrast (top) and fluorescence (bottom) images of the representative mESC colonies are shown. Bars, 100 μm. For LIF− conditions, mESCs were cultured in the absence of LIF for 4 days. Semi-quantitative RT-PCR analysis was performed using cDNAs derived from OGR1 mESCs cultured under LIF+ or LIF− conditions as templates with each gene specific primer set indicated on the right. Ef1α is a positive control. The size of the DNA markers is shown on the left. These results were independently validated by quantitative RT-PCR (Supplementary Fig. 3).

vertebrates, three orthologs of *Drosophila* Hh, i.e., *Desert hedgehog* (*Dhh*), *Indian hedgehog* (*Ihh*) and *Sonic hedgehog* (*Shh*), have unique roles in embryonic development [62–67]. *Shh* is the most broadly expressed ortholog and is involved in embryogenesis, organogenesis and the maintenance of adult stem cells [68]. Without the Shh ligand, the Shh receptor, Patched (Ptch), represses another membrane-bound receptor, Smoothened (Smo). In mammals, two Ptch isoforms, Ptch1 and 2, exist, although Ptch1 is mainly involved in the Hh signaling pathway [69]. When Shh binds to Ptch, Shh represses Ptch, allowing the activation of Smo. Subsequently, Smo can activate the protein activity of transcription factors Gli1, Gli2 and Gli3. Gli2 is the main modulator of the Shh signal [70–72]. Gli3 mostly acts as a transcriptional repressor [73].

In accordance with this knowledge, genes involved in the Hh signaling pathway, except for *Gli2* and *Ptch1*, (*Cdk1, Crebbp, Dhh, Dyrk1a, Gas1, Gli1, Gli3, Igf2, Ihh, Ptch2, Rab23, Sap18, Shh, Sin3a, Ski, Smo, Stk36* and *Sufu*, according to ConPath Navigator) were either constitutively expressed or downregulated in puromycin-positive OVW4 cultures ("puro+"). Furthermore, many of these genes were upregulated when a forced downregulation of *Oct3/4* was induced (*Crebbp, Dyrk1a, Dhh, Sap18, Rab23, Gli3, Sufu* and *Cdk1*; Fig. 4A) or when LIF was withdrawn from the culture (*Gas1, Ski, Igf2, Smo, Ptch1* and *Ptch2*; Fig. 4A). In contrast to these results, our expression microarray analysis showed that *Gli2* and *Ptch1* were consistently highly expressed in mESCs with high transcriptional activity of *Oct3/4*.

To further validate our expression microarray analysis, we examined the expression of selected genes in the Hh signaling pathway (Fig. 4B) in undifferentiated and differentiated mESCs by sqRT-PCR (Fig. 4C). For this analysis, we used a bulk preparation of OGR1 mESCs [27,33,34,37,42] (see Fig. 2) that were maintained under culture conditions with animal serum in the presence or absence of LIF for 4 days. Although significant downregulation of EGFP fluorescence was observed in OGR1 maintained without LIF for 4 days (Fig. 4C "LIF+" on the left vs. "LIF−" on the middle), EGFP fluorescence did not become fully undetectable under these conditions.

We found that undifferentiated mESCs expressed *Gli1, Gli2, Smo* and *Ptch1* (Fig. 4C right). However, the endogenous expression of *Shh* was not detected, which is consistent with the fact that *Gli2* can be expressed in the absence of a Shh signal [71,72]. The expression of *Gli1, Gli2* and *Ptch1* was downregulated 4 days after differentiation of mESCs were induced, whereas the expression of *Gli3* and *Smo* was upregulated (Fig. 4C, see Supplementary Fig. 3 for quantitative results). Because the increased transcription of *Gli1* and *Ptch1* serves as an indicator of Hh pathway activity [69,74,75], it is suggested with these results that Shh signaling was stimulated in undifferentiated mESCs, but not in mESCs cultured in the absence of LIF for 4 days. Interestingly, when mESCs were maintained under chemically-defined serum-free (CDSF) conditions [33,52], we observed downregulation of *Gli1, Gli2* and *Ptch1* (data not shown) in these mESCs. Therefore, animal serum may provide a stimulus to activate the Hh-mediated signal. However, when recombinant Shh was supplemented in a CDSF medium, it failed to provide any significant impact on the growth of mESCs (data not shown). Similarly, endogenous activation of the Hh signal was detected in undifferentiated human ESCs, although exogenously supplied SHH played no significant role in their self-renewal and pluripotency [76]. The self-renewal of human ESCs is dependent on the TGFβ and bFGF signals [77,78], which are known to interact with the Shh signal [79,80]. Therefore, it is suggested with these observations that the Hh-mediated signaling may originate from TGFβ and/or bFGF-like activity in animal serum.

Next, we investigated whether the genes involved in the Hh pathway were expressed in other mouse pluripotent stem cells. The mouse teratocarcinoma cell lines F9 (derived from the testis [35]) and P19 (derived from postimplantation embryos [36]) consistently expressed *Gli2, Smo* and *Ptch1*, although the expression level of *Gli2* was lower in P19 than in F9 and *Gli1* expression was undetectable in P19 (Fig. 5). We could not detect endogenous expression of Shh in F9 or P19 (Fig. 5). Because *Gli* encodes a transcription factor and, interestingly,

the expression of *Gli2* was consistently detected in all of the pluripotent stem cells examined, it is suggested with these results that *Gli2* may play a novel role in the self-renewal of pluripotent stem cells.

3.4. Gli2 exhibited heterogeneous expression in undifferentiated mouse embryonic stem cells

It is suggested with our expression microarray data that Gli2-positive and Gli2-negative cells may both exist in mESCs maintained under standard conditions. Confocal microscopy confirmed that the Gli2 protein was localized in the nuclei and exhibited a patchy staining pattern (Fig. 6A), and that 89% of Gli2-positive mESCs were undifferentiated and Oct3/4-positive (Fig. 6B). In addition, 50% of mESCs with reduced expression levels of the Oct3/4 protein also exhibited low expression levels of the Gli2 protein (arrowheads in Fig. 6A). Therefore, Gli2 expression patterns are highly correlated with Oct3/4 expression patterns in undifferentiated mESCs. Collectively, we suggest that Gli2 may be involved in the network of transcription factors that sustain mESCs self-renewal and pluripotency. However, Gli2 is expected to play a modulatory role instead of an essential role in mESCs because *Gli2*-deficient embryos exhibited defects in body plans but not in cell differentiation per se [81].

3.5. Forced activation of Gli2 significantly enhanced the proliferation rate of mouse embryonic stem cells

To gain an insight into the role that Gli2 plays in mESCs, the protein-coding sequence of the *Gli2* cDNA was subcloned into a novel expression vector (Fig. 7A) and stably expressed in OGR1 mESCs maintained under standard conditions. This vector allows Gli2 to be expressed as a fusion protein with the human estrogen receptor ERT2 [31,32]. When 4-hydroxytamoxifen (4OHT) is supplemented in the culture, Gli2 fused with ERT2 will be activated and localized to nuclei. In addition, this vector assures us a strong expression level of the transgene by the CAG promoter [82] combined with a translational enhancer [45,83] and a transcriptional enhancer [84]. Furthermore, DsRedT3 [85,86] is linked with the immediate downstream of the transgene by the self-cleaving peptide T2A [51] in this vector (Fig. 7A). Therefore, DsRedT3 fluorescence helps us monitor expression levels of Gli2 in real-time (Fig. 7B).

Nine clones that express Gli2 fused with ERT2 (referred to as Gli2ER hereafter) were used for assays. They exhibited varying levels of DsRedT3 fluorescence, whereas quantitative (q) RT-PCR indicated that on average the expression level of *Gli2* increased 244 (±48.24 s.e.m., n = 7) folds in these Gli2ER clones. Parental OGR1 mESCs were used as a control. When 4OHT was added to standard cultures in the presence of LIF and animal serum for 4 days, Gli2ER clones did not exhibit any appearance of cell differentiation (Fig. 7B) and expressed the SSEA1 antigen [49] (Fig. 7C). In addition, heterogeneity in the transcriptional activity of *Oct3/4* was observed in Gli2ER clones treated with 4OHT (Fig. 7B). This was not due to the forced activation of Gli2ER because most of the Gli2ER cells maintained the expression of both EGFP and DsRedT3 (Fig. 7B). This result indicates that Gli2 does not regulate heterogeneous transcriptional activity of *Oct3/4*. However, Gli2ER clones significantly increased their proliferation rate when maintained in the presence of 4OHT for 4 days (1.59 ± 0.230 s.e.m.-fold increase in the nine Gli2ER clones vs. 1.08 ± 0.0601 s.e.m.-fold increase in OGR1, $p < 0.025$, Fig. 7D). When five Gli2ER clones that exhibited bright DsRedT3 fluorescence (260 ± 71.03 s.e.m.-fold increase in the Gli2 level on average) were selected and independently assayed twice or three times, we consistently observed a similar increase in their proliferation rate (1.47 ± 0.157 s.e.m.-fold increase, n = 11, $p < 0.025$). Finally, using five randomly selected Gli2ER clones that were maintained in the presence or absence of 4OHT for 4 days, expression levels of *Oct3/4*, *Eras* and *Gsk3β* were examined by qRT-PCR (the reason why these genes were chosen is described below). As expected from the results
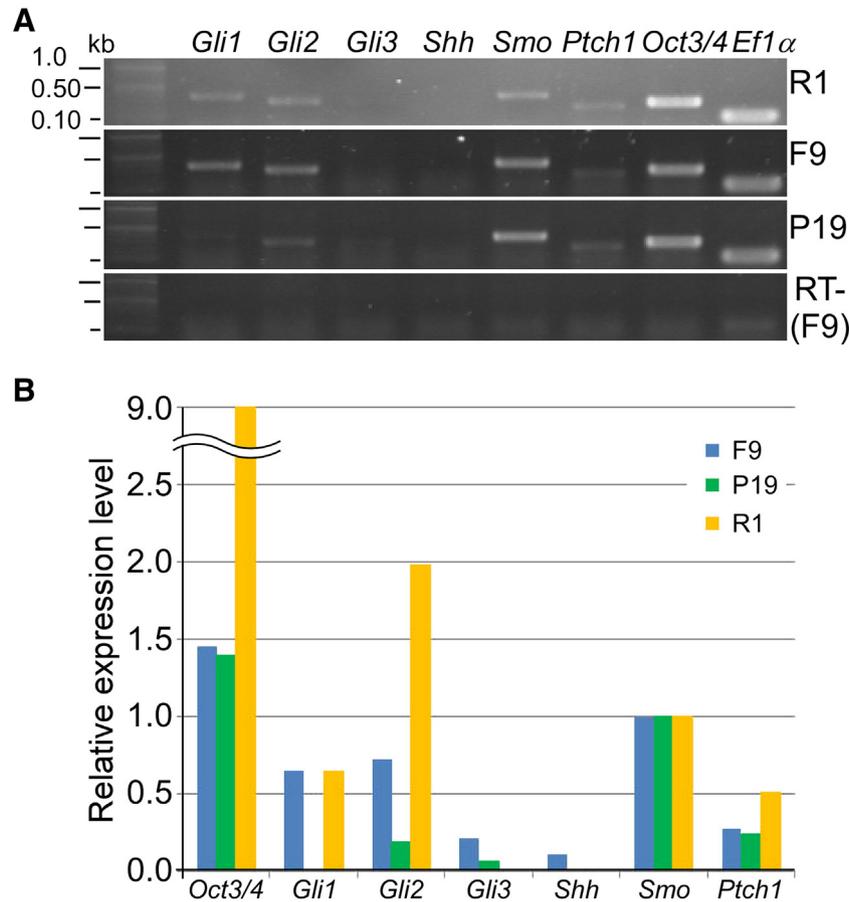
Fig. 5. The expression of genes involved in the Hh pathway in pluripotent stem cells. Semi-quantitative RT-PCR analysis was performed using cDNAs derived from pluripotent stem cells indicated on the right with each gene specific primer set indicated along the top. *Ef1α* is a positive control and RT − is the negative control. The size of the DNA markers is shown on the left. (A) Mouse ESCs (OGR1) and teratocarcinoma cell lines (F9 and P19) were cultured in a standard medium with animal serum. (B) Relative expression levels of genes indicated on the bottom were examined by quantifying mean fluorescence intensities of the PCR products shown in A using ImageJ. *Smo* was used as a reference.

presented in Figs. 7B and C, the expression of *Oct3/4* was stable under these conditions (Fig. 7E). However, the expression level of *Eras* in Gli2ER clones under 4OHT+ conditions decreased to about 40% of the *Eras* level in Gli2ER clones under 4OHT-conditions (Fig. 7E). On the other hand, *Gsk3β* showed a dramatic increase in Gli2ER clones under 4OHT+ conditions (Fig. 7E). Perhaps a positive feedback loop exists
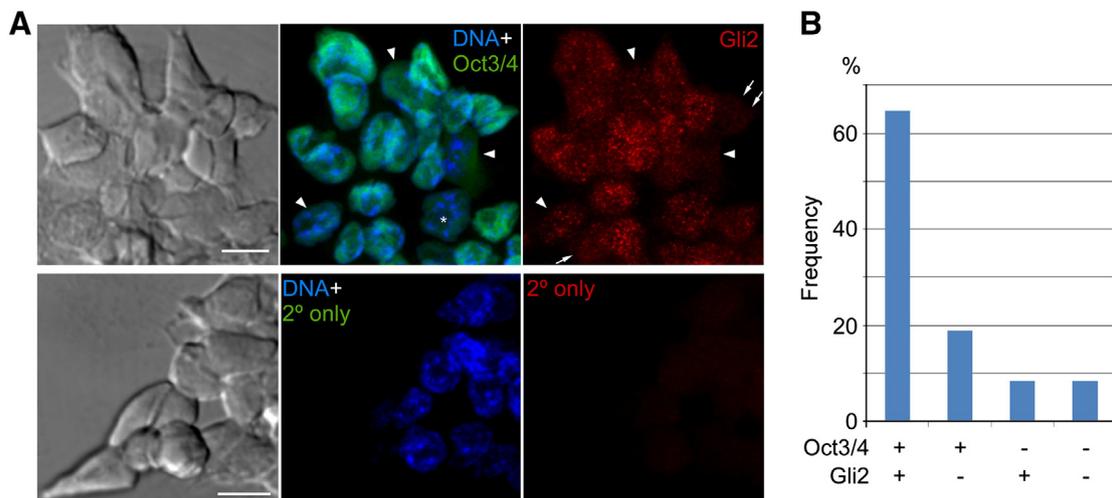

Fig. 6. Oct3/4 and Gli2 are heterogeneously expressed in undifferentiated mESCs. (A) Confocal microscopy was used to examine the localization of Oct3/4 proteins (green; first row, second image), nuclei (blue; first row, second image) and Gli2 proteins (red; first row, third image) in undifferentiated mESCs (first row, first image). Sections were taken every 0.4 μm on the z-axis. Twenty-one sections were stacked and projected for all images. Arrowheads indicate the mESC nuclei with reduced Oct3/4 and Gli2 expression levels. Arrows indicate the mESC nuclei that express Oct3/4, but display reduced expression of Gli2. An asterisk indicates the mESC nuclei with reduced expression of Oct3/4, but expression of Gli2. As a negative control, only secondary antibodies were used ("2° only", second row, second and third images). The nuclear staining of three cells in the bottom left corner of the second row, second image is not visible because these nuclei are out of focus. Bars, 10 μm. (B) The bar chart indicates the frequency (%) of mESC nuclei that show the presence (+) or absence (−) of Oct3/4 and Gli2 expression.
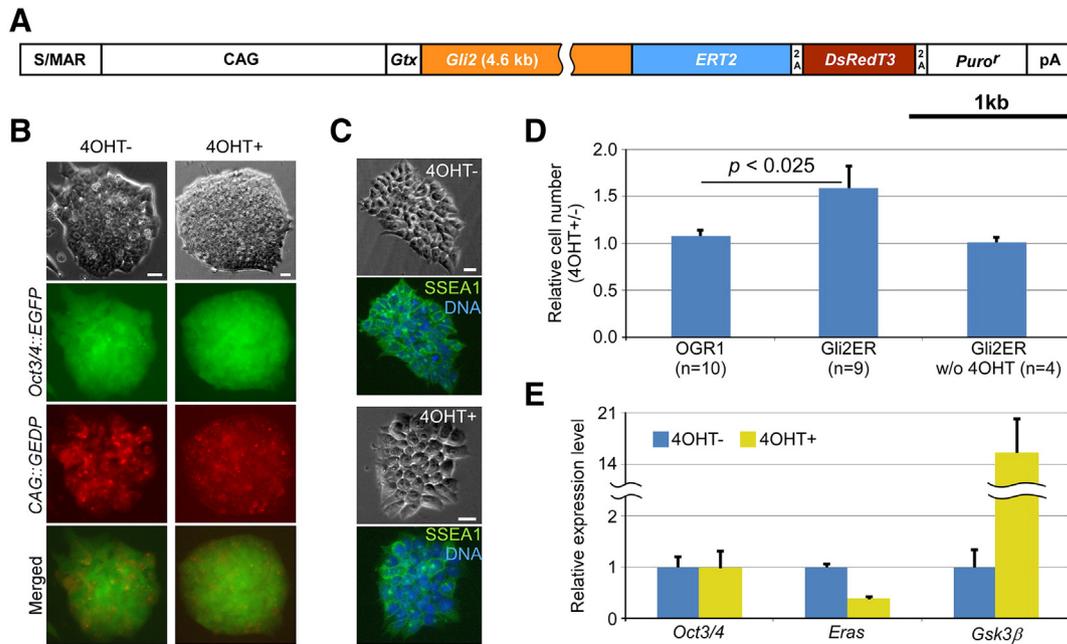
Fig. 7. Forced activation of *Gli2* increased the mESC proliferation rate. (A) A schematic representation of a novel expression vector is shown. Boxes indicate each functional component and are scaled, except for the box of the *Gli2* cDNA [*Gli2* (4.6 kb)]. The bar represents a length of 1 kbp. S/MAR, the synthetic scaffold/matrix associated region motifs [81]; CAG, the CMV enhancer and the chicken β-actin promoter [79]; Gtx, the Gtx motifs [17,80]; ERT2, the human estrogen receptor [30,31]; 2A, the foot-and-mouth disease virus self-cleaving peptide T2A [50]; *DsRedT3*, the DsRedT3 cDNA [82,83]; *Puro*[r], the puromycin N-acetyltransferase gene; pA, the bovine growth hormone polyadenylation signal. (B) Phase contrast (the top row) and fluorescence (the second, third and bottom rows) images representing mESC clones that have the expression vector shown in A stably integrated in the genome and were maintained in the presence (4OHT+) or absence (4OHT−) of 4-hydroxytamoxifen (4OHT) are shown. Fluorescence images shown on the second row indicate transcriptional activity of *Oct3/4* (*Oct3/4::EGFP*), whereas images on the third row indicate transcriptional activity of the transgenes shown in A (*CAG::GEDP*). These green and red fluorescence images are merged on the bottom row. Bars, 20 μm. (C) Phase contrast (the top and third rows) and fluorescence (the second and bottom rows) images of one of the mESC clones maintained with (the third and bottom rows) or without (the top and the second rows) 4OHT are shown. Fluorescence images indicate localization of the SSEA1 antigen (SSEA1, green) and cellular nuclei (DNA, blue). Bars, 20 μm. (D) Mouse ESCs indicated on the bottom were plated in duplicate. Cell numbers in cultures supplemented with 4OHT for 4 days were divided by those without 4OHT. OGR1 was used to generate nine mESC clones (Gli2ER) that have the expression vector shown in A stably integrated. Four Gli2ER clones were plated without 4OHT in duplicate and cell numbers were counted to estimate the plating error (Gli2ER w/o 4OHT). Error bars represent standard errors of the mean. (E) Five Gli2ER clones were randomly chosen to examine relative expression levels of genes indicated on the bottom under conditions with (+, yellow) or without (−, blue) 4OHT. The averaged expression level of each gene under 4OHT− conditions was normalized to 1. *Ef1α* was used as a reference for the $2^{-\Delta\Delta Ct}$ method. Error bars represent standard errors of the mean.

between Gsk3β and Gli2 because Gli2 is one of the Gsk3β substrates and targeted on proteasome-mediated processing [87].

3.6. The possible role that Gli2 plays in mouse embryonic stem cells

Gli1 was initially identified due to its amplification in human glioblastomas [88]. Two homologues of *Gli1*, *Gli2* and *Gli3*, were also expressed in human glioblastomas [89]. The overexpression of *Gli2* in the skin of transgenic mice induced the development of basal cell carcinomas, which are the most common skin tumors in Caucasians [90]. In addition, the overexpression of *GLI2* in a human prostate epithelial cell line resulted in growth acceleration and cell cycle progression [91]. Therefore, it is possible to speculate that *Gli2* may be involved in the tumor-like growth of ESCs.

The tumor-like growth of mESCs is dependent on the activity of *Eras* via the activation of *Akt1* [92]. Because *Akt1* inactivates *Gsk3β* [93–95] and *Gsk3β* inhibits *c-Myc* (*Myc*) [93,96], *Eras* may indirectly activate *c-Myc*, which subsequently drives the self-renewal of mESCs [97]. However, human *ERAS* is not expressed in human ESCs [98,99]. Therefore, we hypothesize that other genetic factors drive the tumor-like growth of both mouse and human ESCs. Interestingly, our data showed that Gli2ER clones significantly increased their proliferation rate (Fig. 7D) while they decreased the expression level of *Eras* (Fig. 7E) under 4OHT+ conditions. Although it needs to be addressed whether the interaction between *Gli2* and *Eras* is direct and whether a feedback loop exist between *Eras* and *Gsk3β* or not, we suggest with our data that *Gli2* may be involved in the tumor-like growth of ESCs.

We recently demonstrated that mESCs cultured under chemically defined serum-free conditions downregulated *Eras* and *c-Myc* and failed to grow into teratomas [33]. Interestingly, mESCs maintained under serum-free conditions restored their tumor-like growth without the upregulation of *Eras* and *c-Myc* when the culture was supplemented with a Gsk3β inhibitor [33]. Therefore, this result strongly supports our hypothesis that other genetic factors are involved in promoting the tumor-like growth of ESCs. Because the serum-free culture provides a unique platform to screen genetic factors responsible for teratoma development in mESCs, further study using this culture system may identify the role of *Gli2* in the tumor-like growth of mESCs.

4. Conclusions

A standard culture of mESCs contains a cell population with reduced *Oct3/4* transcriptional activity, which leads to the generation of subpopulations with expression profiles that are similar to differentiated cells. Heterogeneity in the transcriptional activity of *Oct3/4* was dynamic. Oct3/4 plays an essential role in maintaining basal cellular transcriptional activities while suppressing the expression of genes involved in cell differentiation. The expression of *Gli2*, *Ptch1* and *Smo* was consistently detected in pluripotent stem cells examined in this study. Gli2 expression patterns are highly correlated with Oct3/4 expression patterns in undifferentiated mESCs. Forced activation of *Gli2* in mESCs increased their proliferation rate. It is suggested with our results that *Gli2* may play a novel role in the self-renewal of pluripotent stem cells.

Description of additional data files

"Li_etal_SupInfo.docx" provides a list of primer sets used in this study (Supplementary Table 1), supplementary figures 1, 2 and 3, and supplementary materials and methods.

"Li_et_al_SupTable2.pdf" provides a list of 4,606 differentially 501 expressed genes (Supplementary Table 2). Supplementary data related to this article can be found online at: http://dx.doi.org/10.1016/j.ygeno.2013.09.004.

Competing interests

All authors declare no competing interest.

Authors' contributions

Conception and design: YL, TST. Data collection: YL, TA, TST. Data analysis: YL, JD, RM, TST. Contribution to reagents/materials/analysis tools: DL, MB, FW, RM, TST. Manuscript preparation: YL, MB, RM, TST.

Acknowledgments

References

[1] H. Niwa, K. Ogawa, D. Shimosato, K. Adachi, A parallel circuit of LIF signalling pathways maintains pluripotency of mouse ES cells, Nature 460 (2009) 118–122.

[2] Q.L. Ying, J. Wray, J. Nichols, L. Batlle-Morera, B. Doble, J. Woodgett, P. Cohen, A. Smith, The ground state of embryonic stem cell self-renewal, Nature 453 (2008) 519–523.

[3] I. Chambers, J. Silva, D. Colby, J. Nichols, B. Nijmeijer, M. Robertson, J. Vrana, K. Jones, L. Grotewold, A. Smith, Nanog safeguards pluripotency and mediates germline development, Nature 450 (2007) 1230–1234.

[4] A.M. Singh, T. Hamazaki, K.E. Hankowski, N. Terada, A heterogeneous expression pattern for Nanog in embryonic stem cells, Stem Cells 25 (2007) 2534–2542.

[5] Y. Toyooka, D. Shimosato, K. Murakami, K. Takahashi, H. Niwa, Identification and characterization of subpopulations in undifferentiated ES cell culture, Development 135 (2008) 909–918.

[6] M.G. Carter, C.A. Stagg, G. Falco, T. Yoshikawa, U.C. Bassey, K. Aiba, L.V. Sharova, N. Shaik, M.S. Ko, An in situ hybridization-based screen for heterogeneously expressed genes in mouse ES cells, Gene Expr. Patterns 8 (2008) 181–198.

[7] B. Payer, S.M. Chuva de Sousa Lopes, S.C. Barton, C. Lee, M. Saitou, M.A. Surani, Generation of stella-GFP transgenic mice: a novel tool to study germ cell development, Genesis 44 (2006) 75–83.

[8] T. Furusawa, M. Ikeda, F. Inoue, K. Ohkoshi, T. Hamano, T. Tokunaga, Gene expression profiling of mouse embryonic stem cell subpopulations, Biol. Reprod. 75 (2006) 555–561.

[9] T. Furusawa, K. Ohkoshi, C. Honda, S. Takahashi, T. Tokunaga, Embryonic stem cells expressing both platelet endothelial cell adhesion molecule-1 and stage-specific embryonic antigen-1 differentiate predominantly into epiblast cells in a chimeric embryo, Biol. Reprod. 70 (2004) 1452–1457.

[10] G. Falco, S.-L. Lee, I. Stanghellini, U.C. Bassey, T. Hamatani, M.S.H. Ko, Zscan4: a novel gene expressed exclusively in late 2-cell embryos and embryonic stem cells, Dev. Biol. 307 (2007) 539–550.

[11] M. Zalzman, G. Falco, L.V. Sharova, A. Nishiyama, M. Thomas, S.L. Lee, C.A. Stagg, H.G. Hoang, H.T. Yang, F.E. Indig, R.P. Wersto, M.S. Ko, Zscan4 regulates telomere elongation and genomic stability in ES cells, Nature 464 (2010) 858–863.

[12] A. Suzuki, A. Raya, Y. Kawakami, M. Morita, T. Matsui, K. Nakashima, F.H. Gage, C. Rodriguez-Esteban, J.C. Belmonte, Maintenance of embryonic stem cell pluripotency by Nanog-mediated reversal of mesoderm specification, Nat. Clin. Pract. Cardiovasc. Med. 3 (Suppl. 1) (2006) S114–S122.

[13] A. Suzuki, A. Raya, Y. Kawakami, M. Morita, T. Matsui, K. Nakashima, F.H. Gage, C. Rodriguez-Esteban, J.C. Izpisua Belmonte, Nanog binds to Smad1 and blocks bone

[14] M.A. Canham, A.A. Sharov, M.S. Ko, J.M. Brickman, Functional heterogeneity of embryonic stem cells revealed through translational amplification of an early endodermal transcript, PLoS Biol. 8 (2010) e1000379.

[15] K. Hayashi, S.M. Lopes, F. Tang, M.A. Surani, Dynamic equilibrium and heterogeneity of mouse pluripotent stem cells with distinct functional and epigenetic states, Cell Stem Cell 3 (2008) 391–401.

[16] O.R. Davies, C.Y. Lin, A. Radzisheuskaya, X. Zhou, J. Taube, G. Blin, A. Waterhouse, A.J. Smith, S. Lowell, Tcf15 primes pluripotent cells for differentiation, Cell Rep. 3 (2013) 472–484.

[17] T.S. Tanaka, R.E. Davey, Q. Lan, P.W. Zandstra, W.L. Stanford, Development of a gene-trap vector with a highly sensitive fluorescent protein reporter system for expression profiling, Genesis 46 (2008) 347–356.

[18] A. Filipczyk, K. Gkatzis, J. Fu, P.S. Hoppe, K. Lickert, K. Anastassiadis, T. Schroeder, Biallelic expression of nanog protein in mouse embryonic stem cells, Cell Stem Cell 13 (2013) 12–13.

[19] Y. Li, T.S. Tanaka, Self-renewal, pluripotency and tumorigenesis in pluripotent stem cells revisited, in: C. Atwood (Ed.), Embryonic Stem Cells — Recent Advances in Pluripotent Stem Cell-Based Regenerative Medicine, InTech, 2011, pp. 339–358.

[20] T.S. Tanaka, Transcriptional heterogeneity in mouse embryonic stem cells, Reprod. Fertil. Dev. 21 (2009) 67–75.

[21] T. Graf, M. Stadtfeld, Heterogeneity of embryonic and adult stem cells, Cell Stem Cell 3 (2008) 480–483.

[22] S. Huang, Non-genetic heterogeneity of cells in development: more than just noise, Development 136 (2009) 3853–3862.

[23] A.D. Bolzan, Chromosomal aberrations involving telomeres and interstitial telomeric sequences, Mutagenesis 27 (2012) 1–15.

[24] R.T. Hagelstrom, K.B. Blagoev, L.J. Niedernhofer, E.H. Goodwin, S.M. Bailey, Hyper telomere recombination accelerates replicative senescence and may promote premature aging, Proc. Natl. Acad. Sci. U. S. A. 107 (2010) 15768–15773.

[25] P. Navarro, N. Festuccia, D. Colby, A. Gagliardi, N.P. Mullin, W. Zhang, V. Karwacki-Neisius, R. Osorno, D. Kelly, M. Robertson, I. Chambers, OCT4/SOX2-independent Nanog autorepression modulates heterogeneous Nanog gene expression in mouse ES cells, EMBO J. 31 (2012) 4547–4562.

[26] K.E. Galvin-Burgess, E.D. Travis, K.E. Pierson, J.L. Vivian, TGF-beta-superfamily signaling regulates embryonic stem cell heterogeneity: self-renewal as a dynamic and regulated equilibrium, Stem Cells 31 (2013) 48–58.

[27] F. Chowdhury, Y. Li, Y.-C. Poh, T. Yokohama-Tamaki, N. Wang, T.S. Tanaka, Soft substrates promote homogeneous self-renewal of embryonic stem cells via downregulating cell-matrix tractions, PLoS ONE 5 (2010) e15655.

[28] D. Huh, J. Paulsson, Random partitioning of molecules at cell division, Proc. Natl. Acad. Sci. U. S. A. 108 (2011) 15004–15009.

[29] D. Huh, J. Paulsson, Non-genetic heterogeneity from stochastic partitioning at cell division, Nat. Genet. 43 (2011) 95–100.

[30] T. Nagai, K. Ibata, E.S. Park, M. Kubota, K. Mikoshiba, A. Miyawaki, A variant of yellow fluorescent protein with fast and efficient maturation for cell-biological applications, Nat. Biotechnol. 20 (2002) 87–90.

[31] R. Feil, J. Brocard, B. Mascrez, M. LeMeur, D. Metzger, P. Chambon, Ligand-activated site-specific recombination in mice, Proc. Natl. Acad. Sci. U. S. A. 93 (1996) 10887–10890.

[32] M.E. McLaughlin, G.M. Kruger, K.L. Slocum, D. Crowley, N.A. Michaud, J. Huang, M. Magendantz, T. Jacks, The Nf2 tumor suppressor regulates cell–cell adhesion during tissue fusion, Proc. Natl. Acad. Sci. U. S. A. 104 (2007) 3261–3266.

[33] Y. Li, T. Yokohama-Tamaki, T.S. Tanaka, Short-term serum-free culture reveals that inhibition of Gsk3beta induces the tumor-like growth of mouse embryonic stem cells, PLoS ONE 6 (2011) e21355.

[34] C. Liu, P. Tsai, A.M. Garcia, B. Logeman, T.S. Tanaka, A possible role of Reproductive Homeobox 6 in primordial germ cell differentiation, Int. J. Dev. Biol. 55 (2011) 909–916.

[35] E.G. Bernstine, M.L. Hooper, S. Grandchamp, B. Ephrussi, Alkaline phosphatase activity in mouse teratoma, Proc. Natl. Acad. Sci. U. S. A. 70 (1973) 3899–3903.

[36] M.W. McBurney, B.J. Rogers, Isolation of male embryonal carcinoma cells and their chromosome replication patterns, Dev. Biol. 89 (1982) 503–508.

[37] F. Chowdhury, S. Na, D. Li, Y.C. Poh, T.S. Tanaka, F. Wang, N. Wang, Material properties of the cell dictate stress-induced spreading and differentiation in embryonic stem cells, Nat. Mater. 9 (2010) 82–88.

[38] T.S. Tanaka, K. Ikenishi, Possible role of the 38 kDa protein, lacking in the gastrula-arrested Xenopus mutant, in gastrulation, Dev. Growth Differ. 44 (2002) 23–33.

[39] T.S. Tanaka, T. Tatsuta, K. Ikenishi, Characterization and localization of trupomyosin proteins in Xenopus embryos with specific antibodies, Dev. Growth Differ. 37 (1995) 111–122.

[40] Y. Benjamini, Y. Hochberg, Controlling the false discovery rate: a practical and powerful approach to multiple testing, J. R. Stat. Soc. Ser. B Methodol. 57 (1995) 289–300.

[41] A.I. Saeed, V. Sharov, J. White, J. Li, W. Liang, N. Bhagabati, J. Braisted, M. Klapa, T. Currier, M. Thiagarajan, A. Sturn, M. Snuffin, A. Rezantsev, D. Popov, A. Ryltsov, E. Kostukovich, I. Borisovsky, Z. Liu, A. Vinsavich, V. Trush, J. Quackenbush, TM4: a free, open-source system for microarray data management and analysis, Biotechniques 34 (2003) 374–378.

[42] E. Walker, M. Ohishi, R.E. Davey, W. Zhang, P.A. Cassar, T.S. Tanaka, S.D. Der, Q. Morris, T.R. Hughes, P.W. Zandstra, W.L. Stanford, Prediction and testing of novel transcriptional networks regulating embryonic stem cell self-renewal and commitment, Cell Stem Cell 1 (2007) 71–86.

[43] R. Matoba, H. Niwa, S. Masui, S. Ohtsuka, M.G. Carter, A.A. Sharov, M.S. Ko, Dissecting oct3/4-regulated gene networks in embryonic stem cells by expression profiling, PLoS ONE 1 (2006) e26.

[44] D. Martin, C. Brun, E. Remy, P. Mouren, D. Thieffry, B. Jacq, GOToolbox: functional analysis of gene datasets based on Gene Ontology, Genome Biol. 5 (2004) R101.

[45] T.S. Tanaka, R.E. Davey, Q. Lan, P.W. Zandstra, W.L. Stanford, Development of a gene trap vector with a highly-sensitive fluorescent protein reporter system aiming for the real-time single cell expression profiling, Genesis 46 (2008) 347–356.

[46] T.S. Tanaka, F. Nishiumi, T. Komiya, K. Ikenishi, Characterization of the 38 kDa protein lacking in gastrula-arrested mutant *Xenopus* embryos, Int. J. Dev. Biol. 54 (2010) 1347–1353.

[47] T.S. Tanaka, T. Kunath, W.L. Kimber, S.A. Jaradat, C.A. Stagg, M. Usuda, T. Yokota, H. Niwa, J. Rossant, M.S. Ko, Gene expression profiling of embryo-derived stem cells reveals candidate genes associated with pluripotency and lineage specificity, Genome Res. 12 (2002) 1921–1928.

[48] J. Nichols, B. Zevnik, K. Anastassiadis, H. Niwa, D. Klewe-Nebenius, I. Chambers, H. Scholer, A. Smith, Formation of pluripotent stem cells in the mammalian embryo depends on the POU transcription factor Oct4, Cell 95 (1998) 379–391.

[49] D. Solter, B.B. Knowles, Monoclonal antibody defining a stage-specific mouse embryonic antigen (SSEA-1), Proc. Natl. Acad. Sci. U. S. A. 75 (1978) 5565–5569.

[50] Y.I. Yeom, G. Fuhrmann, C.E. Ovitt, A. Brehm, K. Ohbo, M. Gross, K. Hubner, H.R. Scholer, Germline regulatory element of Oct-4 specific for the totipotent cycle of embryonal cells, Development 122 (1996) 881–894.

[51] A.L. Szymczak, C.J. Workman, Y. Wang, K.M. Vignali, S. Dilioglou, E.F. Vanin, D.A.A. Vignali, Correction of multi-gene deficiency in vivo using a single 'self-cleaving' 2A peptide-based retroviral vector, Nat. Biotechnol. 22 (2004) 589–594.

[52] M. Furue, T. Okamoto, Y. Hayashi, H. Okochi, M. Fujimoto, Y. Myoishi, T. Abe, K. Ohnuma, G.H. Sato, M. Asashima, J.D. Sato, Leukemia inhibitory factor as an anti-apoptotic mitogen for pluripotent mouse embryonic stem cells in a serum-free medium without feeder cells, In Vitro Cell. Dev. Biol. Anim. 41 (2005) 19–28.

[53] R. Raz, C.K. Lee, L.A. Cannizzaro, P. d'Eustachio, D.E. Levy, Essential role of STAT3 for embryonic stem cell pluripotency, Proc. Natl. Acad. Sci. U. S. A. 96 (1999) 2846–2851.

[54] Y.H. Loh, Q. Wu, J.L. Chew, V.B. Vega, W. Zhang, X. Chen, G. Bourque, J. George, B. Leong, J. Liu, K.Y. Wong, K.W. Sung, C.W. Lee, X.D. Zhao, K.P. Chiu, L. Lipovich, V.A. Kuznetsov, P. Robson, L.W. Stanton, C.L. Wei, Y. Ruan, B. Lim, H.H. Ng, The Oct4 and Nanog transcription network regulates pluripotency in mouse embryonic stem cells, Nat. Genet. 38 (2006) 431–440.

[55] J. Nichols, A. Smith, Pluripotency in the embryo and in culture, Cold Spring Harb. Perspect. Biol. 4 (2012) a008128.

[56] K.D. Dahlquist, N. Salomonis, K. Vranizan, S.C. Lawlor, B.R. Conklin, GenMAPP, a new tool for viewing and analyzing microarray data on biological pathways, Nat. Genet. 31 (2002) 19–20.

[57] Y. Nakatake, S. Fujii, S. Masui, T. Sugimoto, S. Torikai-Nishikawa, K. Adachi, H. Niwa, Kinetics of drug selection systems in mouse embryonic stem cells, BMC Biotechnol. 13 (2013) 64.

[58] D.A. Faddah, H. Wang, A.W. Cheng, Y. Katz, Y. Buganim, R. Jaenisch, Single-cell analysis reveals that expression of nanog is biallelic and equally variable as that of other pluripotency factors in mouse ESCs, Cell Stem Cell 13 (2013) 23–29.

[59] K. Hailesellasse Sene, C.J. Porter, G. Palidwor, C. Perez-Iratxeta, E.M. Muro, P.A. Campbell, M.A. Rudnicki, M.A. Andrade-Navarro, Gene function in early mouse embryonic stem cell differentiation, BMC Genomics 8 (2007) 85.

[60] S. Meyer, J. Nolte, L. Opitz, G. Salinas-Riester, W. Engel, Pluripotent embryonic stem cells and multipotent adult germline stem cells reveal similar transcriptomes including pluripotency-related genes, Mol. Hum. Reprod. 16 (2010) 846–855.

[61] P.W. Ingham, A.P. McMahon, Hedgehog signaling in animal development: paradigms and principles, Genes Dev. 15 (2001) 3059–3087.

[62] M.J. Bitgood, L. Shen, A.P. McMahon, Sertoli cell signaling by desert hedgehog regulates the male germline, Curr. Biol. 6 (1996) 298–304.

[63] H.H. Yao, C. Tilmann, G.Q. Zhao, B. Capel, The battle of the sexes: opposing pathways in sex determination, Novartis Found. Symp. 244 (2002) 187–198. discussion 198–206, 253–187.

[64] M. Wijgerde, M. Ooms, J.W. Hoogerbrugge, J.A. Grootegoed, Hedgehog signaling in mouse ovary: Indian hedgehog and desert hedgehog from granulosa cells induce target gene expression in developing theca cells, Endocrinology 146 (2005) 3558–3566.

[65] M.A. Dyer, S.M. Farrington, D. Mohn, J.R. Munday, M.H. Baron, Indian hedgehog activates hematopoiesis and vasculogenesis and can respecify prospective neurectodermal cell fate in the mouse embryo, Development 128 (2001) 1717–1730.

[66] G.R. van den Brink, Hedgehog signaling in development and homeostasis of the gastrointestinal tract, Physiol. Rev. 87 (2007) 1343–1375.

[67] A. Vortkamp, K. Lee, B. Lanske, G.V. Segre, H.M. Kronenberg, C.J. Tabin, Regulation of rate of cartilage differentiation by Indian hedgehog and PTH-related protein, Science 273 (1996) 613–622.

[68] M. Varjosalo, J. Taipale, Hedgehog: functions and mechanisms, Genes Dev. 22 (2008) 2454–2472.

[69] S.W. Choy, S.H. Cheng, Hedgehog signaling, Vitam. Horm. 88 (2012) 1–23.

[70] C.B. Bai, W. Auerbach, J.S. Lee, D. Stephen, A.L. Joyner, Gli2, but not Gli1, is required for initial Shh signaling and ectopic activation of the Shh pathway, Development 129 (2002) 4753–4761.

[71] C.B. Bai, A.L. Joyner, Gli1 can rescue the in vivo function of Gli2, Development 128 (2001) 5161–5172.

[72] A. Ruiz i Altaba, Combinatorial Gli gene function in floor plate and neuronal inductions by sonic hedgehog, Development 125 (1998) 2203–2212.

[73] A. Ruiz i Altaba, C. Mas, B. Stecca, The Gli code: an information nexus regulating cell fate, stemness and cancer, Trends Cell Biol. 17 (2007) 438–447.

[74] A. Shaw, J. Gipp, W. Bushman, The sonic hedgehog pathway stimulates prostate tumor growth by paracrine signaling and recapitulates embryonic gene expression in tumor myofibroblasts, Oncogene 28 (2009) 4480–4490.

[75] C.J. Tabin, A.P. McMahon, Recent advances in hedgehog signalling, Trends Cell Biol. 7 (1997) 442–446.

[76] S.M. Wu, A.B. Choo, M.G. Yap, K.K. Chan, Role of sonic hedgehog signaling and the expression of its components in human embryonic stem cells, Stem Cell Res. 4 (2010) 38–49.

[77] T.E. Ludwig, V. Bergendahl, M.E. Levenstein, J. Yu, M.D. Probasco, J.A. Thomson, Feeder-independent culture of human embryonic stem cells, Nat. Methods 3 (2006) 637–646.

[78] T.E. Ludwig, M.E. Levenstein, J.M. Jones, W.T. Berggren, E.R. Mitchen, J.L. Frane, L.J. Crandall, C.A. Daigh, K.R. Conard, M.S. Piekarczyk, R.A. Llanas, J.A. Thomson, Derivation of human embryonic stem cells in defined conditions, Nat. Biotechnol. 24 (2006) 185–187.

[79] S. Dennler, J. Andre, I. Alexaki, A. Li, T. Magnaldo, P. ten Dijke, X.J. Wang, F. Verrecchia, A. Mauviel, Induction of sonic hedgehog mediators by transforming growth factor-beta: Smad3-dependent activation of Gli2 and Gli1 expression in vitro and in vivo, Cancer Res. 67 (2007) 6981–6986.

[80] A. Pirskanen, J.C. Kiefer, S.D. Hauschka, IGFs, insulin, Shh, bFGF, and TGF-beta1 interact synergistically to promote somite myogenesis in vitro, Dev. Biol. 224 (2000) 189–203.

[81] R. Mo, A.M. Freer, D.L. Zinyk, M.A. Crackower, J. Michaud, H.H. Heng, K.W. Chik, X.M. Shi, L.C. Tsui, S.H. Cheng, A.L. Joyner, C. Hui, Specific and redundant functions of Gli2 and Gli3 zinc finger genes in skeletal patterning and development, Development 124 (1997) 113–123.

[82] H. Niwa, K. Yamamura, J. Miyazaki, Efficient selection for high-expression transfectants with a novel eukaryotic vector, Gene 108 (1991) 193–199.

[83] S.A. Chappell, G.M. Edelman, V.P. Mauro, A 9-nt segment of a cellular mRNA can function as an internal ribosome entry site (IRES) and when present in linked multiple copies greatly enhances IRES activity, Proc. Natl. Acad. Sci. U. S. A. 97 (2000) 1536–1541.

[84] J. Bode, Y. Kohwi, L. Dickinson, T. Joh, D. Klehr, C. Mielke, T. Kohwi-Shigematsu, Biological significance of unwinding capability of nuclear matrix-associating DNAs, Science 255 (1992) 195–197.

[85] K. Vintersten, C. Monetti, M. Gertsenstein, P. Zhang, L. Laszlo, S. Biechele, A. Nagy, Mouse in red: red fluorescent protein expression in mouse ES cells, embryos, and adult animals, Genesis 40 (2004) 241–246.

[86] B.J. Bevis, B.S. Glick, Rapidly maturing variants of the *Discosoma* red fluorescent protein (DsRed), Nat. Biotechnol. 20 (2002) 83–87.

[87] J. Jiang, Regulation of Hh/Gli signaling by dual ubiquitin pathways, Cell Cycle 5 (2006) 2457–2463.

[88] K.W. Kinzler, J.M. Ruppert, S.H. Bigner, B. Vogelstein, The GLI gene is a member of the Kruppel family of zinc finger proteins, Nature 332 (1988) 371–374.

[89] V. Clement, P. Sanchez, N. de Tribolet, I. Radovanovic, A. Ruiz i Altaba, HEDGEHOG-GLI1 signaling regulates human glioma growth, cancer stem cell self-renewal, and tumorigenicity, Curr. Biol. 17 (2007) 165–172.

[90] M. Grachtchouk, R. Mo, S. Yu, X. Zhang, H. Sasaki, C.C. Hui, A.A. Dlugosz, Basal cell carcinomas in mice overexpressing Gli2 in skin, Nat. Genet. 24 (2000) 216–217.

[91] S. Thiyagarajan, N. Bhatia, S. Reagan-Shaw, D. Cozma, A. Thomas-Tikhonenko, N. Ahmad, V.S. Spiegelman, Role of GLI2 transcription factor in growth and tumorigenicity of prostate cells, Cancer Res. 67 (2007) 10642–10646.

[92] K. Takahashi, K. Mitsui, S. Yamanaka, Role of ERas in promoting tumour-like properties in mouse embryonic stem cells, Nature 423 (2003) 541–545.

[93] M. Bechard, S. Dalton, Subcellular localization of glycogen synthase kinase 3beta controls embryonic stem cell self-renewal, Mol. Cell. Biol. 29 (2009) 2092–2104.

[94] D. Wu, W. Pan, GSK3: a multifaceted kinase in Wnt signaling, Trends Biochem. Sci. 35 (2010) 161–168.

[95] D.A. Cross, D.R. Alessi, P. Cohen, M. Andjelkovich, B.A. Hemmings, Inhibition of glycogen synthase kinase-3 by insulin mediated by protein kinase B, Nature 378 (1995) 785–789.

[96] T.C. He, A.B. Sparks, C. Rago, H. Hermeking, L. Zawel, L.T. da Costa, P.J. Morin, B. Vogelstein, K.W. Kinzler, Identification of c-MYC as a target of the APC pathway, Science 281 (1998) 1509–1512.

[97] P. Cartwright, C. McLean, A. Sheppard, D. Rivett, K. Jones, S. Dalton, LIF/STAT3 controls ES cell self-renewal and pluripotency by a Myc-dependent mechanism, Development 132 (2005) 885–896.

[98] T. Kameda, J.A. Thomson, Human ERas gene has an upstream premature polyadenylation signal that results in a truncated, noncoding transcript, Stem Cells 23 (2005) 1535–1540.

[99] Y. Tanaka, T. Ikeda, Y. Kishi, S. Masuda, H. Shibata, K. Takeuchi, M. Komura, T. Iwanaka, S. Muramatsu, Y. Kondo, K. Takahashi, S. Yamanaka, Y. Hanazono, ERas is expressed in primate embryonic stem cells but not related to tumorigenesis, Cell Transplant. 18 (2009) 381–389.